NANO LETTERS

2008
Vol. 8, No. 1
323−327

Transparent, Conductive Graphene Electrodes for Dye-Sensitized Solar Cells

Xuan Wang, Linjie Zhi,* and Klaus Müllen*

Max Planck Institute for Polymer Research, Ackermannweg 10, D-55128 Mainz, Germany

Received October 31, 2007; Revised Manuscript Received November 19, 2007

ABSTRACT

Transparent, conductive, and ultrathin graphene films, as an alternative to the ubiquitously employed metal oxides window electrodes for solid-state dye-sensitized solar cells, are demonstrated. These graphene films are fabricated from exfoliated graphite oxide, followed by thermal reduction. The obtained films exhibit a high conductivity of 550 S/cm and a transparency of more than 70% over 1000–3000 nm. Furthermore, they show high chemical and thermal stabilities as well as an ultrasmooth surface with tunable wettability.

Indium tin oxide (ITO) and fluorine tin oxide (FTO) have been widely used as window electrodes in optoelectronic devices.[1] These metal oxides, however, appear to be increasingly problematic due to (i) the limited availability of the element indium on earth, (ii) their instability in the presence of acid or base, (iii) their susceptibility to ion diffusion into polymer layers, (iv) their limited transparency in the near-infrared region, and (v) the current leakage of FTO devices caused by FTO structure defects.[2] The search for novel electrode materials with good stability, high transparency and excellent conductivity is therefore a crucial goal for optoelectronics.[3] Graphene, two-dimensional graphite, as a rising star in material science, exhibits remarkable electronic properties that qualify it for applications in future optoelectronic devices.[4] Recently, transparent and conductive graphene-based composites have been prepared by incorporation of graphene sheets into polystyrene or silica.[5] However, the conductivity of such transparent composites is low, typically ranging from 10^{-3} to 1 S/cm depending upon the graphene sheet loading level, which makes the composites incapable of serving as window electrodes in optoelectronic devices.

Herein, we present a simple approach for the fabrication of conductive, transparent, and ultrathin graphene films from exfoliated graphite oxide, followed by thermal reduction. The obtained graphene films with a thickness of ca. 10 nm exhibit a high conductivity of 550 S/cm, which is comparable to that of polycrystalline graphite (1250 S/cm), and a transparency of more than 70% over 1000−3000 nm. The application of graphene films as window electrodes in solid-state dye-sensitized solar cells is demonstrated.

* Corresponding authors: E-mail: L.Z., zhi@mpip-mainz.mpg.de; K.M., muellen@mpip-mainz.mpg.de. Telephone: (+49) 6131-379-151. Fax: (+49) 6131-379-350.

10.1021/nl072838r CCC: $40.75 © 2008 American Chemical Society
Published on Web 12/11/2007

Graphene sheets have been produced either by mechanical exfoliation *via* repeated peeling of highly ordered pyrolytic graphite (HOPG) or by chemical oxidation of graphite.[6,9] Considering the facile solution processing, the oxidation of graphite was preferred for this study. Oxygen-containing functional groups render the graphite oxide (GO) hydrophilic and dispersible in water.

GO was produced by the Hummers method[6] through acid oxidation of flake graphite. The primary product was suspended in water under ultrasonication for half an hour, followed by centrifuged at 4000 rpm for 30 min. The obtained supernate was dried via evaporation of water under vacuum. Then, the solid were dispersed again in water (1.5 mg/mL) by ultrasonicated for 2 h and centrifuged at 10 000 rpm for 15 min to further remove aggregates. Finally, the supernate was collected and ready for use. Such aqueous dispersion of exfoliated GO could stay stable for several weeks, free of any obvious precipitates. The exfoliated graphene sheets with lateral dimensions of several tens to hundreds of nanometers were observed under scanning electron microscopy (SEM) (Figure 1a). However, the obtained GO are electrically insulating due to the heavy oxygenation of graphene sheets. Reduction of GO, either by chemical reaction using reducing agent,[10] such as $NaBH_4$ or dimethylhydrazine, or by pyrolysis at high temperatures,[11] has been reported to render the material electrically conductive. However, to avoid agglomeration of graphene sheets after reduction, other host molecules such as polymers must be used,[5,10] which hamper the electron-transfer property of the graphenes. In this work, GO sheets were first deposited on the surface of the substrate and then reduced into graphenes, which afforded ultrathin and homogeneous graphene films.

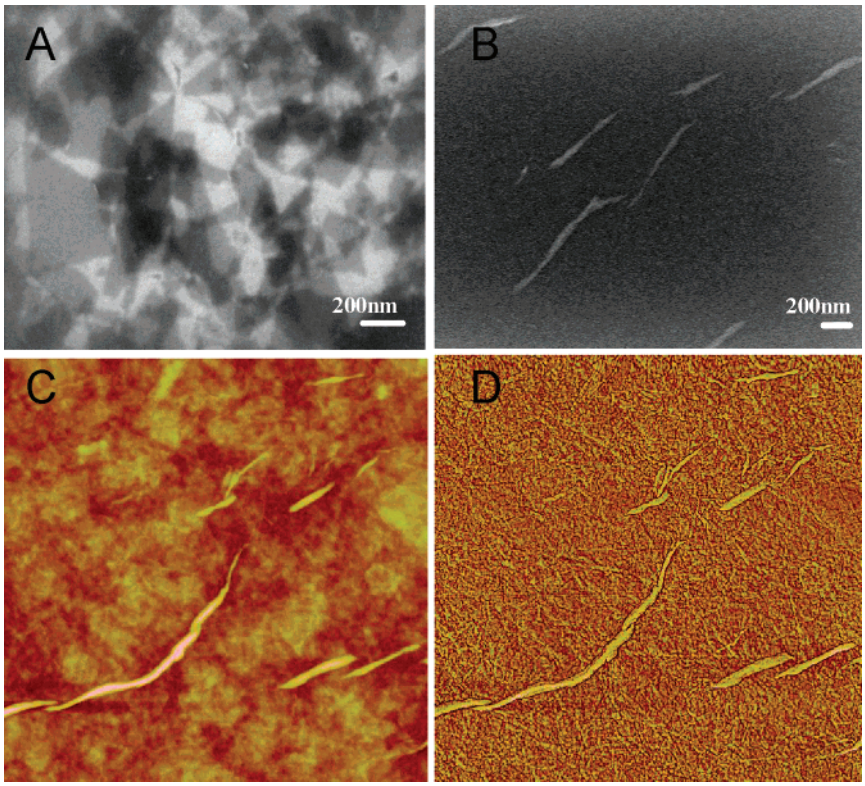

Figure 1. Morphology of GO films. (A) SEM image of exfoliated graphite oxide (GO). (B) SEM image of GO film prepared from dip coating. (C) AFM height image (3.2 × 3.2 μm^2) (color scale: black to bright yellow, 30 nm). (D) AFM phase image (color scale: black to bright yellow, 15°) of the obtained GO film.

Typically, GO sheets were deposited on hydrophilic substrates (such as pretreated quartz) by dip coating of a hot, aqueous GO dispersion and subsequent temperature-controlled drying of the film. The thickness of the film was tuned by changing the temperature of GO dispersion as well as the dipping repetition. For example, 2-fold dip coating of the GO dispersion at 70 °C resulted in a ca. 10 nm thick, continuous and homogeneous film. Quasi-one-dimensional creases with a length of 0.2−2.5 μm and a height of 5−20 nm were observed with SEM (Figure 1b) and atomic force microscopy (AFM), which was formed by the overlap of GO sheets where some of the graphene edges were scrolled or folded[12] (Figure 1c,d) during film fabrication.

Reduction of the GO film into a graphene film was achieved *via* thermal treatment under protection of Ar and/or H_2 flow. Color change from light brown to light gray of the GO film on quartz indicated the formation of graphene. The obtained graphene film displayed similar morphology to GO film and creases were occasionally observed (Supporting Information). However, the surface roughness (R_a) has been improved significantly after thermal treatment. The average R_a of the as prepared graphene film over a 10 × 10 μm^2 area is ca. 0. 78 nm. It is widely accepted that the R_a of the electrodes is crucial in optoelectronic devices.[2] In contrast to the rough FTO surface,[13] which might short-circuit the cells, an ultrasmooth surface is a prominent characteristic of the graphene films.

The electrical conductivity of the as-prepared graphene films is closely related to the annealing temperature and the thickness of the film. At a given film thickness of ca. 10 nm, concomitant increase of film conductivity was observed with an increase in the heating temperatures from 550 to 1100 °C (Supporting Information). The sheet resistance (R_s) of a 10.1 ± 0.76 nm thick graphene film prepared by 1100 °C thermal treatment was 1.8 ± 0.08 kΩ/sq using a four-point probe method (at 20 different positions of the film), and the calculated average conductivity is ca. 550 S/cm. In addition, the conductivity of graphene film increased to 727 S/cm when the film thickness was increased to 29.9 ± 1.1 nm, for which the R_s is 0.46 ± 0.03 kΩ/sq. The high conductivity of the graphene film, comparable to that of polycrystalline graphite (1250 S/cm),[14] results from the effective recovering and subsequent annealing of continuous and overlapped graphene sheets by removal of oxygenated groups in GO films as shown by IR spectroscopy (Supporting Information).

Raman spectra of the graphene film (obtained at 1100 °C) showed two typical bands at 1598 cm^{-1} (G band) and 1300 cm^{-1} (D band) (Supporting Information), similar to that of conventional carbon nanotubes.[15] The crystalline lattice of the graphenes is visible under high-resolution transmission electron micrograph (HRTEM). Typically, two crystal planes corresponding to *d*-spacing of 0.216 nm {indices $(0\bar{1}10)$} and 0.126 nm {indices $(1\bar{2}10)$} were found by selected-area electron diffraction (SAED) (Supporting Information), which is consistent with the results reported for single or double layer graphenes.[12] In some areas of the film, stacking of the graphenes to up to tens of layers was observed (Figure 2a). Two dominant SAED peaks for indices (0002) (0.347 nm spacing) and $(0\bar{1}10)$ (0.218 nm spacing) are very strong in

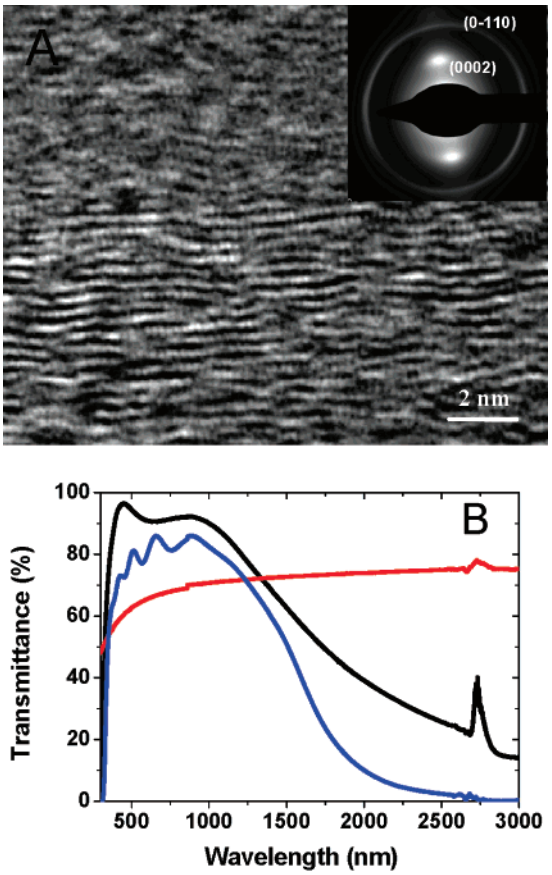

Figure 2. Structure and transmittance of graphene films. (A) HRTEM image of graphene films with corresponding SAED pattern (inset). (B) Transmittance of a ca. 10 nm thick graphene film (red), in comparison with that of ITO (black) and FTO (blue).

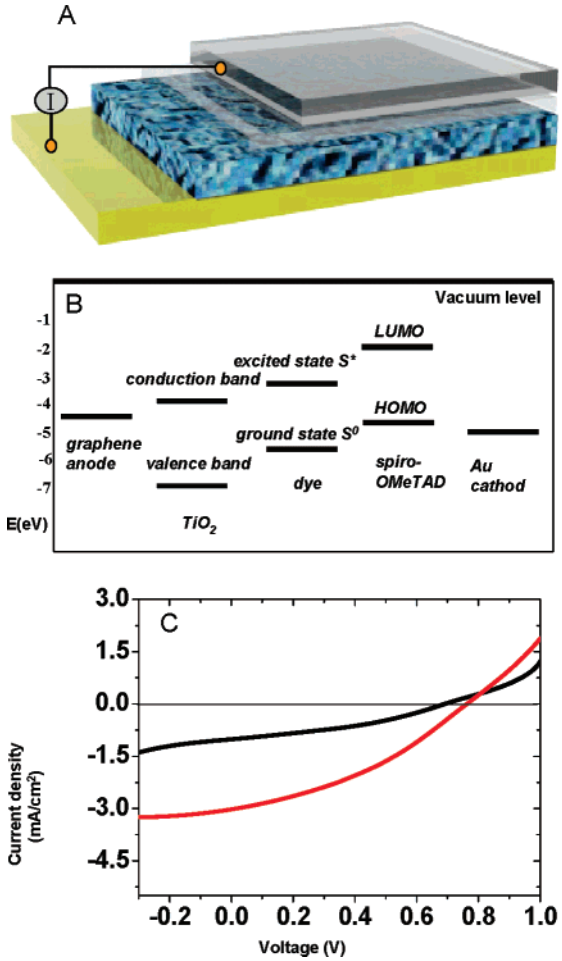

Figure 3. Illustration and performance of solar cell based on graphene electrodes. (A) Illustration of dye-sensitized solar cell using graphene film as electrode, the four layers from bottom to top are Au, dye-sensitized heterojunction, compact TiO_2, and graphene film. (B) The energy level diagram of graphene/TiO_2/dye/spiro-OMeTAD/Au device. (C) *I*−*V* curve of graphene-based cell (black) and the FTO-based cell (red), illuminated under AM solar light (1 sun).

this case, suggesting the existence of scrolled or folded graphenes in the film,[12] which was probably caused by the scratching of the film during TEM sample preparation or by the creases formed during the film fabrication.

The transmittance of the graphene film depends on the film thickness. At a wavelength of 1000 nm, a ca. 10 nm thick film has a transmittance of 70.7%, which is lower than that of FTO (purchased from Solaronix SA, TCO 10−10) of 82.4% and ITO (purchased from Merck KGaA, with an ITO thickness of about 120 nm and sheet sheet resistance $<15\ \Omega\ cm^{-2}$) of 90.0%. However, decreasing the film thickness leads to an improvement of the transmittance to over 80.0%. Most interestingly, in contrast to FTO and ITO, which show strong absorptions in the region of near- (0.75−1.4 μm) and short-wavelength infrared (1.4−3 μm), the graphene films remain transparent in these regions (Figure 2b). This unique optical property makes the graphene films outstanding as window electrodes for optoelectronics applicable to a wide range of wavelengths. Films obtained from lower temperatures such as 700 and 500 °C show stronger absorption in the range 200−1000 nm, compared to the films obtained from 1100 °C (Supporting Information), suggesting that the transparency of graphene films is also correlated to their structures. A higher extent of graphitization of GO film is important to improve not only the transmittance but also the conductivity of the finally formed graphene films.

Besides low resistance, high transparency, and a smooth surface, a high thermal stability is necessary for application as electrodes in dye-sensitized TiO_2 solar cells to replace FTO. After heating to as high as 400 °C in air, the graphene films remain intact and have a conductivity comparable to that of the original films. Furthermore, in contrast to metal oxide coatings, graphene films are chemically stable and resistant to strong acids such as hydrochloride acid. It is also notable that the surface wettability of graphene film is tunable. The contact angle of graphene films was changed from 66.5−69° to 2.2−8.6° by exposure to argon plasma treatment for 30 s. Thereby, the sheet resistance of the film changed little from 0.9 to 1.08 kΩ/sq.

To demonstrate how the transparent graphene films are potential window electrodes for optoelectronics, a dye-sensitized solid solar cell based on spiro-OMeTAD[1] (as a hole transport material) and porous TiO_2 (for electron transport) was fabricated using the graphene film as anode and Au as cathode (Figure 3a). In optoelectronic devices, proper contact between electrode and p/n type material is

essential for charge collection. Figure 3b shows the energy level diagram of a graphene/TiO_2/dye/spiro-OMeTAD/Au device. Because the calculated work function of graphene is 4.42 eV[16] and the mostly reported work function of HOPG is 4.5 eV,[17] it is reasonable to presume that the work function of as prepared graphene film is close to that of FTO electrode (4.4 eV[18]). The electrons are first injected from the excited state of the dye into the conduction band of TiO_2 and then reach the graphene electrode via a percolation mechanism inside the porous TiO_2 structure.[19] Meanwhile, the photo-oxidized dyes are regenerated by the spiro-OMeTAD hole conducting molecules.

Because spiro-OMeTAD and graphite have been proved to form ohmic contact,[19] a blocking TiO_2 layer is used to prohibit the possible recombination of the charge carriers at the interface of graphene electrode/spiro-OMeTAD. Therefore, the devices were prepared by first depositing a compact blocking TiO_2 layer via spin-coating Ti−IV tetra-isopropoxide (TTIP) ethanol solution[7] on electrodes of graphene films or F-doped SnO_2 (FTO, purchased from Solaronix SA). Afterward, the substrate was sintered at 400 °C for 30 min, followed by fabrication of a 2.5−3 μm thick mesoporous film of TiO_2 via doctor-blading a TiO_2 paste (Ti-Nanoxide T, Solaronix). The substrate was sintered at 400 °C again for 1 h and then sensitized by soaking in an ethanol solution of ruthenium dye N3 (Ru(4,4′-dicarboxy-2,2′-bipyridine)$_2$-$(NCS)_2$) for 7 h and then washed with ethanol. The hole transporter matrix layer was prepared by spin-coating a solution of spiro-OMeTAD (0.17 M) in chlorobenzene, containing *tert*-butylpyridine (0.13 M), $N(PhBr)_3SbCl_6$ (0.3 mM), and $Li(CF_3SO_2)_2N$ (0.013 M).[8] Finally, a 50 nm thick Au electrode was evaporated on top of substrates.

The current−voltage ($I-V$) characteristics of the device (the efficient area of the device is 0.11 cm^2) under illumination of simulated solar light (light intensity: 98.3 mW/cm^2, calibrated against silicon photovoltaic solar cells) showed a short-circuit photocurrent density (I_{sc}) of 1.01 mA/cm^2 with an open-circuit voltage (V_{oc}) of 0.7 V, calculated filling factor (FF) of 0.36, and overall power conversion efficiency of 0.26%. For comparison, an FTO-based cell was fabricated and evaluated with the same procedure and device structure by replacing graphene film electrode with FTO. The FTO-based cell gave I_{sc} of 3.02 mA/cm^2, V_{oc} of 0.76 V, FF of 0.36, and an efficiency of 0.84%. The somewhat lower I_{sc} and efficiency of the graphene film-based cell might be possibly due to the series resistance of the device, the relatively lower transmittance of the electrode, as well as the electronic interfacial change. We believe there is room for improvement, such as increasing conductivity of graphene films via the use of graphene sheets with lateral dimensions on the micrometer scale, or exploitation of a new and special structure of solar cells based on graphene films as electrodes. Further investigation of high quality graphene film preparation such as using bottom-up approaches with chemically synthesized nanographenes as precursors and more suitable engineering procedures for fabricating graphene film-based cells is ongoing in our group.

It should be noted that the concept of using transparent, conductive graphene films as window electrodes in solar cells works well, even in a nonoptimized state. The advantages of our approach include cheap and abundant carbon resources and simple fabrication procedures. The unique properties of the as-obtained graphene film [(i) excellent conductivity, (ii) good transparency in both the visible and near-infrared regions, (iii) ultrasmooth surface with tunable wettability, (iv) high chemical and thermal stabilities, and (v) flexibility for transfer between alternative substrates] render the graphene-based window electrodes versatile for applications not only in solar cells described in this work but also in many other optoelectronic devices. Obviously, this is a new starting point in the direction of graphene window electrodes for the development of next generation of optoelectronics. Expectations and exciting discoveries both will be in front of us.

Acknowledgment. This work was financially supported by the Deutsche Forschungsgemeinschaft (SFB 625) and the Max Planck Society through the program ENERCHEM. We thank Dr. C. G. Clark, Jr. for his help in the preparation of the manuscript.

Supporting Information Available: Figure S1. Surface morphology of graphene films. Figure S2. Conductivity (with error bars) of graphene films vs temperatures of pyrolysis. Figure S3. IR spectra of GO and graphene films. Figure S4. HRTEM and ED of graphene films. Figure S5. Raman spectrum of graphene films. Figure S6. Transmittance of graphene films obtained at different temperatures. This material is available free of charge via the Internet at http://pubs.acs.org.

References

(1) (a) Bach, U.; Lupo, D.; Comte, P.; Moser, J. E.; Weissörtel, F.; Salbeck, J.; Spreitzer, H.; Grätzel, M. *Nature* **1998**, *395*, 583. (b) Mende, L. S.; Fechtenkötter, A.; Müllen, K.; Moons, E.; Friend, R. H.; MacKenzie, J. D. *Science* **2001**, *293*, 1119.

(2) (a) Schlatmann, A. R.; Floet, D. W.; Hilberer, A.; Garten, F.; Smulders, P. J. M.; Klapwijk, T. M.; Hadziioannou, G. *Appl. Phys. Lett.* **1996**, *69*, 1764. (b) Scott, J. C.; Kaufman, J. H.; Brock, P. J.; DiPietro, R.; Salem, J.; Goitia, J. A. *J. Appl. Phys.* **1996**, *79*, 2745. (c) Andersson, A.; Johansson, N.; Bröms, P.; Yu, N.; Lupo, D.; Salaneck, W. R. *Adv. Mater.* **1998**, *10*, 859. (d) Wang, L.; Yang, Y.; Marks, T. J.; Liu, Z. F.; Ho, S. T. *Appl. Phys. Lett.* **2005**, *87*, 161107.

(3) (a) Gustafsson, G.; Cao, Y.; Treacy, G. M.; Klavetter, F.; Colaneri, N.; Heeger, A. J. *Nature* **1992**, *357*, 477. (b) Wu, Z. C.; Chen, Z. H.; Du, X.; Logan, J. M.; Sippel, J.; Nikolou, M.; Kamaras, K.; Reynolds, J. R.; Tanner, D. B.; Hebard, A. F.; Rinzler, A. G. *Science* **2004**, *305*, 1273. (c) Cui, J.; Wang, A.; Edleman, N. L.; Ni, J.; Lee, P.; Armstrong, N. R.; Marks, T. J. *Adv. Mater.* **2001**, *13*, 1476. (d) Zhang, M.; Fang, S. L.; Zakhidov, A;, A.; Lee, S. B.; Aliev, A. E.; Williams, C. D.; Atkinson, K. R.; Baughman, R. H. *Science* **2005**, *309*, 1215.

(4) (a) Geim, A. K.; Novoselov, K. S. *Nat. Mater.* **2007**, *6*, 183. (b) Zhang, Y.; Tan, J. W.; Stormer, H. L.; Kim, P. *Nature* **2005**, *438*, 201. (c) Klitzing, K. V.; Dorda, G.; Pepper, M. *Phys. Rev. Lett.* **1980**, *45*, 494. (d) Heersche, H.; Herrero, P. J.; Oostinga, J. B.; Vandersypen, L. M. K.; Morpurgo, A. F. *Nature* **2007**, *446*, 56.

(5) (a) Stankovich, S.; Dikin, D. A.; Dommett, G. H. B.; Kohlhaas, K. M.; Zimney, E. J.; Stach, E. A.; Piner, R. D.; Nguyen, S. T.; Ruoff, R. S. *Nature* **2006**, *442*, 282. (b) Watcharotone, S.; Dikin, D. A.; Stankovich, S.; Piner, R.; Jung, I.; Dommett, G. H. B.; Evmenenko, G.; Wu, S. E.; Chen, S. F.; Liu, C. P.; Nguyen, S. T.; Ruoff, R. S. *Nano Lett.* **2007**, *7*, 1888. (c) Chen, G.; Weng, W.; Wu, D.; Wu, C. *Eur. Polym. J.* **2003**, *39*, 2329.

(6) Hummers, W. S.; Offeman, J. R. E. *J. Am. Chem. Soc*. **1958**, *80*, 1339.
(7) Saito, Y.; Kitamura, T.; Wada, Y.; Yanagida, S. *Synth. Met.* **2002**, *131*, 185.
(8) Mende, L. S.; Grätzel, M. *Thin Solid Films* **2006**, *500*, 296.
(9) (a) Novoselov, K. S.; Geim, A. K.; Morozov, S. V.; Jiang, D.; Zhang, Y.; Dubonos, S. V.; Grigorieva, I. V.; Firsov, A. A. *Science* **2004**, *306*, 666. (b) Niyogi, S.; Bekyarova, E.; Itkis, M. E.; McWilliams, J. L.; Hamon, M. A.; Haddon, R. C. *J. Am. Chem. Soc.* **2006**, *128*, 7720.
(10) (a) Bourlinos, A. B.; Gournis, D.; Petridis, D.; Szabó, T.; Szeri, A.; Dékány, I. *Langmuir* **2003**, *19*, 6050. (b) Stankovich, S.; Piner, R. D.; Chen, X. Q.; Wu, N. Q.; Nguyen, S. T.; Ruoff, R. S. *J. Mater. Chem*. **2006**, *16*, 155.
(11) (a) Matuyama, E. *J. Phys. Chem*. **1954**, *58*, 215. (b) Matuyama, E. *J. Phys. Chem*. **1965**, *69*, 2462. (c) Hirata, M.; Gotou, T.; Ohba, M. *Carbon* **2005**, *43*, 505.
(12) Meyer, J. C.; Geim, A. K.; Katsnelson, M. I.; Novoselov, K. S.; Booth, T. J.; Roth, S. *Nature* **2007**, *446*, 60.
(13) Varshney, P.; Deepa, M.; Sharma, N.; Agnihotry, S. A. *Solid State Ionics* **2002**, *152*−*153*, 877.
(14) Grisdale, R. O. *J. Appl. Phys*. **1953**, *24*, 1288.
(15) Belin, T.; Epron, F. *Mater. Sci. Eng. B* **2005**, *119*, 105.
(16) Czerw, R.; Foley, B.; Tekleab, D.; Rubio, A.; Ajayan, P. M.; Carroll, D. L. *Phys. Rev. B* **2002**, *66*, 033408.
(17) (a) Wildoeer, J. W. G.; Venema, L. C.; Rinzler, A. G.; Smalley, R. E.; Dekker, C. *Nature*, **1998**, *391*, 59. (b) Pellegrinoa, O.; Vilarb, M. R.; Horowitzc, G.; Botelho do Regoa, A. M. *Mater. Sci. Eng. C* **2002**, *22*, 367.
(18) Andersson, A.; Johansson, N.; Bröms, P.; Yu, N.; Lupo, D.; Salaneck, W. R. *Adv. Mater.* **1999**, *10*, 859.
(19) Bach, U. Ph.D. thesis, Swiss Federal Institute of Technology Lausanne, 2000.

NL072838R